

Research Article

Multilayer Full Polarization Conversion Transpolarizing Structures

Misagh Khosronejad , Gian Guido Gentili, and Giuseppe Macchiarella

Department of Electronics, Information and Bioengineering, Politecnico di Milano, Milan 20133, Italy

Correspondence should be addressed to Misagh Khosronejad; misagh.khosronejad@polimi.it

Received 17 December 2018; Accepted 19 February 2019; Published 11 April 2019

Academic Editor: Ikmo Park

Copyright © 2019 Misagh Khosronejad et al. This is an open access article distributed under the Creative Commons Attribution License, which permits unrestricted use, distribution, and reproduction in any medium, provided the original work is properly cited.

In this paper, we propose the design of two perfect multilayered linear transpolarization structures working in transmission. These linear polarization converters are capable to rotate the polarization 90° independently from the direction of the input linear polarization. Results show an excellent conversion ratio.

1. Introduction

Polarization state is one of the fundamental properties of electromagnetic waves. In many telecommunication applications such as fiber-optic communication and remote sensing, it is often required to have a control on the polarization state of wave propagation [1]. Several classic approaches that are well-known are based on birefringent crystals, Faraday rotation, or Brewster angle effects [2]. These approaches in some cases suffer from bulky and heavy structure making them less appealing in modern integrated systems. In the recent decade, several advanced designs were proposed to mitigate such problems [1, 3–6], many of these being based on metasurfaces. Metasurfaces are usually made of periodic structures in which the unit cell is smaller than the operating wavelength. Once the unit cell is suitably designed for a required electromagnetic response, various functional devices can be realized including polarization converters [1, 7–9].

According to literature and possible applications, linear polarization converters might be the most widely used device among various types of polarization converter devices. A linear polarization converter basically can rotate the linear polarization of the incident wave by 90°, making it cross-

polar with respect to that of the incident wave. Due to the importance of such devices, a great amount of research efforts has been carried out by the research community in the recent years in order to study and develop novel devices operating this task [7–14]. In this letter, we propose the design of two multilayered linear polarization (LP) converters in transmission mode. The proposed devices are capable to rotate the linear polarization of incident wave by 90 degrees irrespectively of the direction of the polarization direction of the incident wave.

2. Design of Polarization Converters

In the following, we first provide the basic principles of LP converters and indicate the requirements in order to design LP converters. It was found that a perfect LP conversion device can be achieved once the considered metallic layout breaks the symmetry of the unit cell. Simulation results of the proposed devices show an excellent conversion ratio independently from the incident polarization direction.

Consider an incident linear polarized wave:

$$\vec{E}_{\text{inc}} = (\vec{E}_x + \vec{E}_y) e^{-i\beta z} = |E_0| (\hat{a}_x \cos \varphi + \hat{a}_y \sin \varphi) e^{-i\beta z}. \quad (1)$$

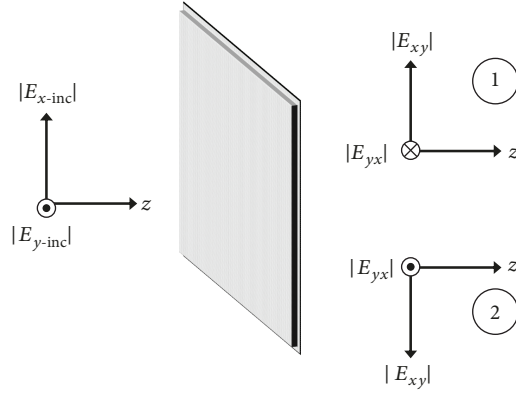
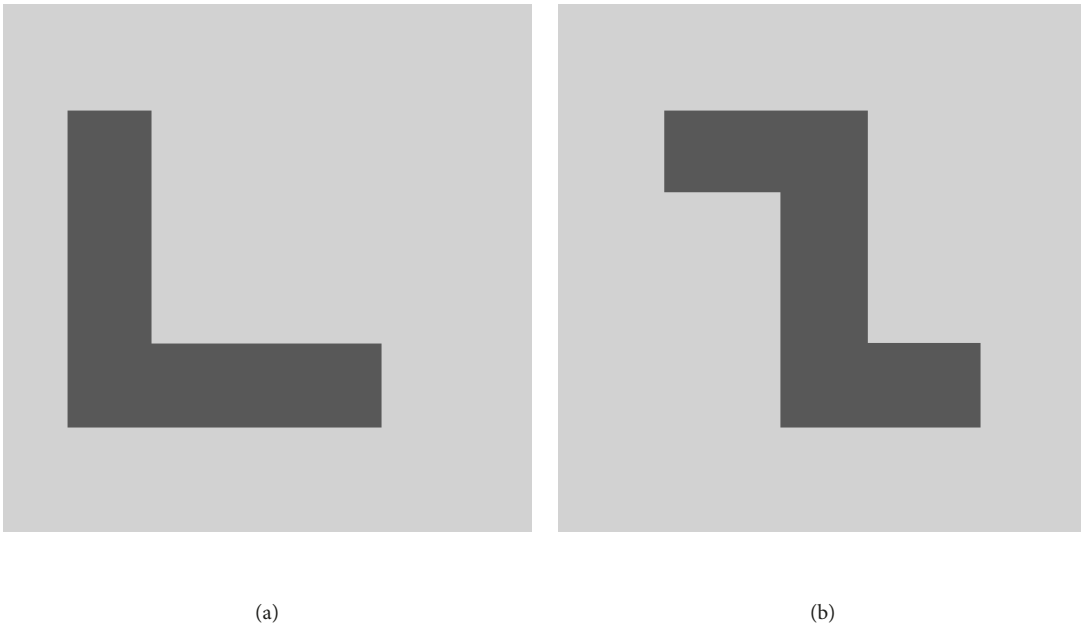


FIGURE 1: Working principles of a linear polarization converter device.

FIGURE 2: Single layer unit cells ($0.43\lambda_0 \times 0.43\lambda_0$) of the two proposed LP converter devices with (a) L and (b) Z configurations.

A perfect linear polarization conversion with 90° rotation of the wave can be achieved, when one of the conditions shown in Figure 1 is satisfied:

$$\vec{E}_t = \pm |E_0| \left[\hat{a}_x \cos \left(\varphi + \frac{\pi}{2} \right) + \hat{a}_y \sin \left(\varphi + \frac{\pi}{2} \right) \right] e^{-i\beta z}. \quad (2)$$

For clarity, equation 2 can be interpreted in such way that realization of a perfect LP converter device requires the maximum conversion of cross-polar components magnitude to each other alongside with 180° phase difference in transmitted components with respect to the incident ones. Up to date, there are several design frameworks for LP converter transmitter surfaces that suffer from either difficult realization of PEMC and metamaterial surfaces [1, 15] or limitation on the polarization direction of the incident wave [16, 17].

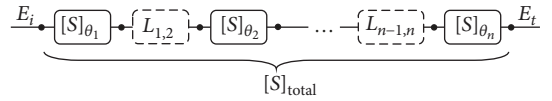


FIGURE 3: A multilayered network schematic.

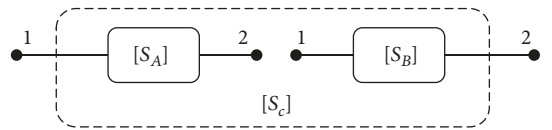


FIGURE 4: Representative picture of two cascaded networks.

Figure 2 depicts two single layer unit cells which are the basis structures of the proposed multilayer LP converters in this work. The unit cells are designed to

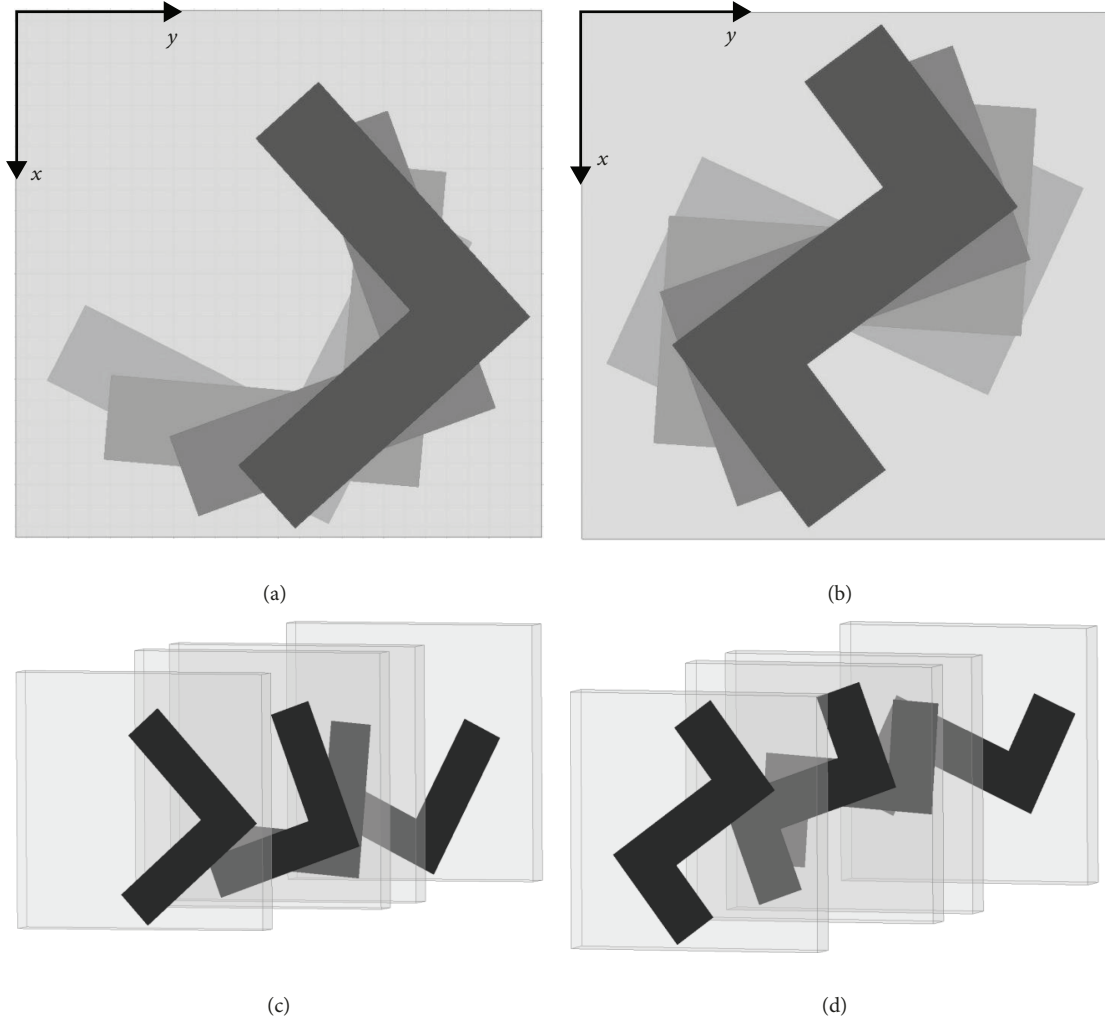


FIGURE 5: A unit cell of the proposed 4-layered perfect LP converters, (a) top view of L, (b) top view of Z, (c) 3D view of L, and (d) 3D view of Z configurations.

TABLE 1: Design parameters of the proposed 4-layered perfect LP converters.

Structure	$\theta_1(^{\circ})$	$\theta_2(^{\circ})$	$\theta_3(^{\circ})$	$\theta_4(^{\circ})$	$L_{1,2}/\lambda_0$	$L_{2,3}/\lambda_0$	$L_{3,4}/\lambda_0$
L	132	110	85	63	0.641	0.151	0.633
Z	127	110	86	65	0.612	0.171	0.609

* θ_i is the rotation angle of the structure in layer i . * L_{ij} is the physical distance between adjacent layers i and j . * λ_0 is the wavelength in free space.

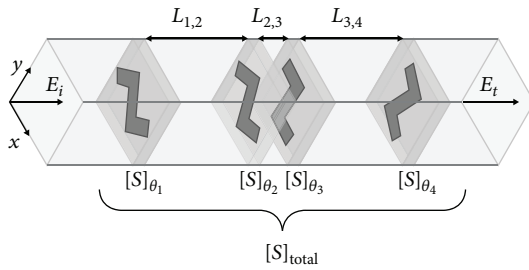


FIGURE 6: 3D view of a 4-layered Z-shaped LP converter.

resonate at the desired operating frequencies and are asymmetrical. Considering the multilayered network shown in Figure 3, one can cascade several rotated layers of the basis structures and obtain a total output scattering matrix satisfying the requested goal.

$$S_{\text{total}} = \begin{bmatrix} [R^{11}] & [T^{12}] \\ [T^{21}] & [R^{22}] \end{bmatrix} = \begin{bmatrix} \begin{bmatrix} r_{xx}^{11} & r_{xy}^{11} \\ r_{yx}^{11} & r_{yy}^{11} \end{bmatrix} & \begin{bmatrix} t_{xx}^{12} & t_{xy}^{12} \\ t_{yx}^{12} & t_{yy}^{12} \end{bmatrix} \\ \begin{bmatrix} t_{xx}^{21} & t_{xy}^{21} \\ t_{yx}^{21} & t_{yy}^{21} \end{bmatrix} & \begin{bmatrix} r_{xx}^{22} & r_{xy}^{22} \\ r_{yx}^{22} & r_{yy}^{22} \end{bmatrix} \end{bmatrix}. \quad (3)$$

In equation 3, R and T indicate reflection and transmission coefficients, respectively, x and y denote perpendicular modes, and the numbers are indicating input/output ports.

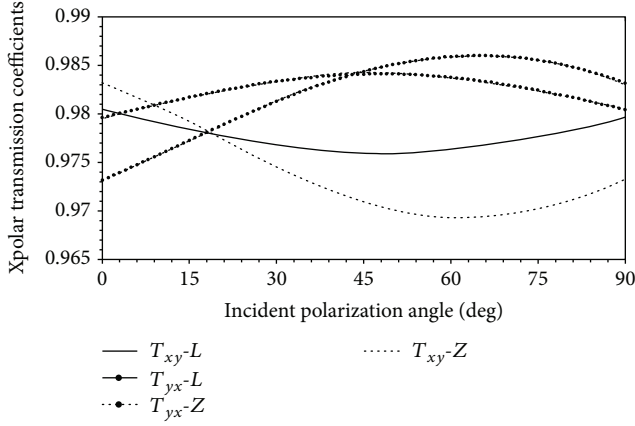


FIGURE 7: Cross-polar transmission coefficients of the proposed 4-layered perfect LP converter devices versus direction of incident wave polarization at resonance frequency.

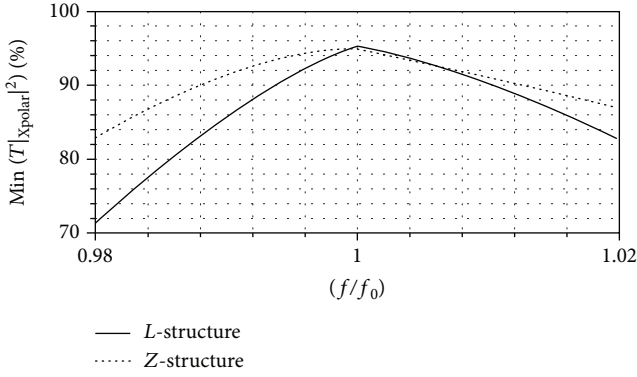


FIGURE 8: Minimum power conversion of the proposed LP converters with respect to the direction of incident wave polarization.

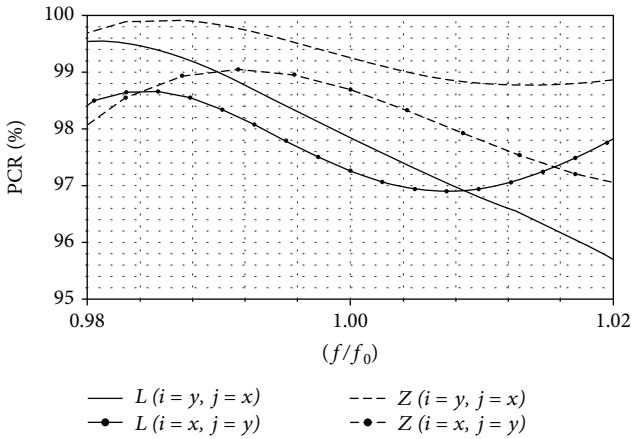


FIGURE 9: The computed PCR of L - and Z -shaped LP converters.

According to reciprocity theorem, the transmission matrices shown in equation 3 are related as

$$[T^{21}] = [T^{12}]^T, \quad (4)$$

so in case of a perfect LP converter device, we must have

$$\begin{cases} |T_{xy}^{21}| = |T_{yx}^{12}| = 1, \\ |T_{yx}^{21}| = |T_{xy}^{12}| = 1. \end{cases} \quad (5)$$

Furthermore, it can be verified that in order to have the polarization conversion not dependent on the direction of the linear polarized incident wave, the following phase condition must be satisfied as well:

$$|\Delta\varphi(T_{yx}^{21}, T_{xy}^{21})| = |\Delta\varphi(T_{yx}^{12}, T_{xy}^{12})| = \pi. \quad (6)$$

Given the scattering matrix of a unit cell structure, it can be demonstrated that the scattering matrix of the rotated structure can be obtained by a suitable combination between two floquet modes. Moreover, the method of cascading the rotated structures is rather simple. Consider $[S_A]$ and $[S_B]$ that represent the scattering matrix of the two reciprocal networks shown in Figure 4.

The equivalent scattering matrix of the cascaded network in Figure 4, $[S_C]$, is obtained as

$$\begin{cases} S_C^{11} = S_A^{11} + S_A^{12} S_B^{11} S_A^{21} (I - S_A^{22} S_B^{11})^{-1}, \\ S_C^{12} = S_A^{12} S_B^{11} S_A^{22} S_B^{12} (I - S_A^{22} S_B^{11})^{-1} + S_A^{12} S_B^{12}, \\ S_C^{21} = S_A^{21} S_B^{11} (I - S_A^{22} S_B^{11})^{-1}, \\ S_C^{22} = S_B^{22} + S_A^{22} S_B^{12} S_B^{21} (I - S_A^{22} S_B^{11})^{-1}, \end{cases} \quad (7)$$

where I indicates a unitary matrix.

Figure 5 illustrates the proposed 4-layered perfect LP converters obtained by cascaded connection of rotated unit cells shown in Figure 2. The rotation angle of the structures and distances between layers is reported in Table 1. Figure 6 shows the design parameters of a 4-layered perfect LP converter in 3D view.

Due to periodicity of the transmission coefficients for all 360° of input polarization direction, Figure 7 illustrates cross-polar transmission coefficients in only one quarter of the angular period. The minimum power conversion ratio of the proposed 4-layered LP converters with respect to the direction of incident wave polarization is reported in Figure 8. Results illustrate more than 90% conversion ratio over the bandwidth of 1.6% and 2.4% (at f_0) for the proposed LP converters with L and Z configuration, respectively. It should be noted that results are shown for structures formed by lossless dielectric substrates with dielectric constant of 4.4 and perfect electric conductors.

To verify the efficiency of 4-layered LP converters, two converters were designed based on L - and Z -unit cells at

resonance frequencies of 10.25 GHz and 11.7 GHz, respectively. The dielectric used in the designs was a 1.6 mm-thick FR4-epoxy with dielectric constant of 4.4 and loss tangent of 0.02. According to Table 1, unit cell dimensions were calculated and simulations were carried out using a commercial code based on the Finite Element Method (Ansys HFSS). Figure 9 illustrates the polarization conversion ratio (PCR) of the proposed LP converters around their resonance frequencies.

$$\text{PCR}_{ji} = \frac{T_{ji}^2}{T_{ji}^2 + T_{ij}^2}, \quad i, j = x, y. \quad (8)$$

3. Conclusions

In conclusion, we presented the design of two linear polarization converters based on the cascaded connection of rotated unit cells. The proposed structures are rotating the input linear polarization by 90° independently from the direction of polarization and achieve an excellent conversion ratio.

Data Availability

No data were used to support this study.

Conflicts of Interest

The authors declare that there is no conflict of interest regarding the publication of this paper.

References

- [1] G. Zhou, X. Tao, Z. Shen et al., “Designing perfect linear polarization converters using perfect electric and magnetic conducting surfaces,” *Scientific Reports*, vol. 6, no. 1, article 38925, 2016.
- [2] E. Hecht, *Optics*, Pearson Education, 2002.
- [3] S. Sun, Q. He, S. Xiao, Q. Xu, X. Li, and L. Zhou, “Gradient-index meta-surfaces as a bridge linking propagating waves and surface waves,” *Nature Materials*, vol. 11, no. 5, pp. 426–431, 2012.
- [4] J. P. B. Mueller, K. Leosson, and F. Capasso, “Ultracompact metasurface in-line polarimeter,” *Optica*, vol. 3, no. 1, pp. 42–47, 2016.
- [5] V. V. Klimov, I. V. Zabkov, A. A. Pavlov, R. C. Shiu, H. C. Chan, and G. Y. Guo, “Manipulation of polarization and spatial properties of light beams with chiral metafilms,” *Optics Express*, vol. 24, no. 6, pp. 6172–6185, 2016.
- [6] R. Verre, N. Maccaferri, K. Fleischer et al., “Polarization conversion-based molecular sensing using anisotropic plasmonic metasurfaces,” *Nanoscale*, vol. 8, no. 20, pp. 10576–10581, 2016.
- [7] Y. Ye and S. He, “90° polarization rotator using a bilayered chiral metamaterial with giant optical activity,” *Applied Physics Letters*, vol. 96, no. 20, article 203501, 2010.
- [8] Y. J. Chiang and T. J. Yen, “A composite-metamaterial-based terahertz-wave polarization rotator with an ultrathin thickness, an excellent conversion ratio and enhanced transmission,” *Applied Physics Letters*, vol. 102, no. 1, article 011129, 2013.
- [9] N. K. Grady, J. E. Heyes, D. R. Chowdhury et al., “Terahertz metamaterials for linear polarization conversion and anomalous refraction,” *Science*, vol. 340, no. 6138, pp. 1304–1307, 2013.
- [10] K. Song, Y. Liu, Q. Fu, X. Zhao, C. Luo, and W. Zhu, “90° polarization rotator with rotation angle independent of substrate permittivity and incident angles using a composite chiral metamaterial,” *Optics Express*, vol. 21, no. 6, pp. 7439–7446, 2013.
- [11] H. Shi, A. Zhang, S. Zheng, J. Li, and Y. Jiang, “Dual-band polarization angle independent 90° polarization rotator using twisted electric-field-coupled resonators,” *Applied Physics Letters*, vol. 104, no. 3, article 034102, 2014.
- [12] S. C. Jiang, X. Xiong, Y. S. Hu et al., “Controlling the polarization state of light with a dispersion-free metastructure,” *Physical Review X*, vol. 4, no. 2, article 021026, 2014.
- [13] Z. H. Jiang, L. Lin, D. Ma et al., “Broadband and wide field-of-view plasmonic metasurface-enabled waveplates,” *Scientific Reports*, vol. 4, no. 1, p. 7511, 2014.
- [14] L. Cong, W. Cao, X. Zhang et al., “A perfect metamaterial polarization rotator,” *Applied Physics Letters*, vol. 103, no. 17, article 171107, 2013.
- [15] H. M. El-Maghrabi, A. M. Attiya, and E. Hashish, “Design of a perfect electromagnetic conductor (PEMC) boundary by using periodic patches,” *Progress in Electromagnetics Research M*, vol. 16, pp. 159–169, 2011.
- [16] N. K. Grady, J. E. Heyes, D. R. Chowdhury et al., “Broadband and high-efficiency terahertz metamaterial linear polarization converters,” in *2013 38th International Conference on Infrared, Millimeter, and Terahertz Waves (IRMMW-THz)*, pp. 1–3, Germany, September 2013.
- [17] Y. Xu, X. Liu, Z. Zhu, Z. Wang, and J. Shi, “Linear polarization conversion in planar chiral metamaterial,” in *2013 International Conference on Optoelectronics and Microelectronics (ICOM)*, pp. 245–247, China, September 2013.



Hindawi

Submit your manuscripts at
www.hindawi.com

